

Dif1 Controls Subcellular Localization of Ribonucleotide Reductase by Mediating Nuclear Import of the R2 Subunit[∇]

Xiaorong Wu and Mingxia Huang*

Department of Biochemistry and Molecular Genetics, University of Colorado School of Medicine, Aurora, Colorado 80045

Received 3 September 2008/Returned for modification 11 September 2008/Accepted 24 September 2008

Fidelity in DNA replication and repair requires adequate and balanced deoxyribonucleotide pools that are maintained primarily by regulation of ribonucleotide reductase (RNR). RNR is controlled via transcription, protein inhibitor association, and subcellular localization of its two subunits, R1 and R2. *Saccharomyces cerevisiae* Sml1 binds R1 and inhibits its activity, while *Schizosaccharomyces pombe* Spd1 impedes RNR holoenzyme formation by sequestering R2 in the nucleus away from the cytoplasmic R1. Here we report the identification and characterization of *S. cerevisiae* Dif1, a regulator of R2 nuclear localization and member of a new family of proteins sharing separate homologous domains with Spd1 and Sml1. Dif1 is localized in the cytoplasm and acts in a pathway different from the nuclear R2-anchoring protein Wtm1. Like Sml1 and Spd1, Dif1 is phosphorylated and degraded in cells encountering DNA damage, thereby relieving inhibition of RNR. A shared domain between Sml1 and Dif1 controls checkpoint kinase-mediated phosphorylation and degradation of the two proteins. Abolishing Dif1 phosphorylation stabilizes the protein and delays damage-induced nucleus-to-cytoplasm redistribution of R2. This study suggests that Dif1 is required for nuclear import of the R2 subunit and plays an essential role in regulating the dynamic RNR subcellular localization.

Maintenance of genomic stability depends on faithful replication of DNA and repair of lesions after damage. Fidelity of both DNA replication and repair is influenced by perturbation in the sizes and relative ratios of cellular deoxynucleotide triphosphate (dNTP) pools. Ribonucleotide reductase (RNR) catalyzes the essential step of converting ribonucleoside diphosphates to the corresponding deoxy forms and is largely responsible for maintaining cellular dNTP pools (34). As maximal DNA synthesis requires high concentrations of dNTPs, the RNR activity plays an important role in cell proliferation (31). On the other hand, increased RNR activity has been associated with malignant transformation and resistance to chemotherapy (12, 14, 25, 56).

The class I RNR holoenzymes are commonly found in eukaryotes and eubacteria and comprise two subunits, R1 and R2 (34). The active site and multiple binding sites for allosteric effectors reside in R1 (20), which can exist as a dimer, tetramer, and hexamer depending on the nucleotides present and their concentrations (21, 37, 47). R2 is a homodimer or heterodimer that houses a diferric-tyrosyl radical cofactor [(Fe)₂-Y] essential for nucleotide reduction (36, 40, 42). Mammalian genomes contain a single R1 gene and two R2 genes; the cell cycle-regulated RRM2 is responsible for providing dNTPs in actively dividing cells, and the DNA damage-inducible p53R2 is required for replenishing dNTP pools in cells under genotoxic stress (9, 22, 44). Loss of p53R2 causes mitochondrial DNA depletion and increased apoptosis (22). The budding yeast *Saccharomyces cerevisiae* has two R1 genes, *RNR1* and *RNR3*. *RNR1* is essential for mitotic growth, while *RNR3* is

highly inducible after DNA damage but dispensable for cell viability. The yeast R2 is a heterodimer of Rnr2 and Rnr4 (17, 36, 41). Only Rnr2 is capable of forming the (Fe)₂-Y' cofactor (36). Rnr4 is incapable of forming any radical, as it contains substitutions in three of the six conserved residues required for iron binding (17, 35, 48). Nevertheless, Rnr4 is required to facilitate the generation of radicals in Rnr2 and stabilizes the resulting heterodimer both in vitro and in vivo (7, 36, 46).

Because of its central role in generation and maintenance of dNTP pools, the RNR enzyme is subjected to complex regulation both in cells going through normal cell cycle progression and in cells (resting or proliferating) encountering genotoxic stress. RNR concentrations and activity can be modulated at the level of transcription, protein inhibitor interaction, and protein degradation, as well as subcellular localization, all of which are under the control of the DNA damage and replication checkpoint kinases ATR/Mec1 and CHK2/Rad53. Transcription of the mammalian p53R2 gene is induced by UV irradiation in a p53-dependent manner (32, 44). In *S. cerevisiae*, DNA damage and replication blockage induce transcription of three of the four *RNR* genes (*RNR2* to *RNR4*) through checkpoint kinase-mediated phosphorylation and removal of the transcriptional repressor Crt1 from its target promoters (18). The *S. cerevisiae* genome encodes the 104-residue protein Sml1 that binds and inhibits the R1 subunit (8, 54). Sml1 is an unstable protein and undergoes checkpoint-dependent phosphorylation and degradation during S phase of the cell cycle and in cells experiencing genotoxic stress (52, 55). Although no apparent sequence homolog of Sml1 has been identified in multicellular organisms, Sml1 can bind the mammalian R1 and inhibits its activity (8, 53), suggesting a conserved mechanism of Sml1-R1 interaction and inhibition.

Dynamic change in subcellular localization patterns of the R2 subunit offers another major mode of RNR regulation. In both *S. cerevisiae* and *Schizosaccharomyces pombe*, R1 is con-

* Corresponding author. Mailing address: Department of Biochemistry and Molecular Genetics, University of Colorado School of Medicine, Aurora, CO 80045. Phone: (303) 724-3204. Fax: (303) 724-3215. E-mail: mingxia.huang@uchsc.edu.

[∇] Published ahead of print on 6 October 2008.

stitutively localized in the cytoplasm, whereas R2 is predominantly localized in the nucleus except for S phase of the cell cycle, when R2 becomes colocalized with R1 in the cytoplasm (29, 50). Upon DNA damage or replication blockage, R2 is redistributed from the nucleus to the cytoplasm in a checkpoint-dependent manner, leading to colocalization of R1 and R2 (29, 50). A similar dynamic change in RNR subunit subcellular localization has also been reported in plant cells and mammalian cells (28, 30), although it is unclear whether the mechanistic details of the localization changes are conserved throughout evolution. In *S. cerevisiae*, the heterodimeric R2 subunit Rnr2-Rnr4 is cotransported between the nucleus and the cytoplasm (2). Proper nuclear localization of R2 requires the WD40 protein Wtm1, which acts as a nuclear anchor of R2, and the karyopherin Kap122, which is involved in importing Wtm1 into the nucleus (26, 51). Subcellular localization of *S. pombe* R2 is controlled by the 127-residue protein Spd1 (29). Spd1 was originally identified in a screen for S-phase inhibitors because its overexpression causes G₁ arrest (49). Spd1 is subjected to checkpoint-dependent phosphorylation and proteolysis in response to DNA damage (4, 29). Its destruction has been found to correlate with redistribution of R2 from the nucleus to the cytoplasm (29, 43). Overexpression of Spd1 retains R2 in the nucleus even in the presence of DNA damage. Thus, Spd1 likely acts as a nuclear anchor of R2 (29).

The *S. pombe* Spd1 and *S. cerevisiae* Sml1 proteins share no sequence homology despite their similarities in protein sizes, functional roles in RNR inhibition, and regulation by the checkpoint kinases. Sml1 inhibits RNR through binding of the R1 subunit, whereas Spd1 inhibits RNR through sequestration of the R2 subunit in the nucleus away from R1. Interestingly, purified recombinant Spd1 protein has been shown to bind the *S. pombe* R1 subunit and inhibits its activity *in vitro*, while Spd1-R2 interaction cannot be detected under the same conditions (16). However, the measured specific activity of purified *S. pombe* R1 in the report (~ 10 nmol dCDP/mg/min [16]) is extremely low relative to that of the *S. cerevisiae* R1 (250 nmol dCDP/mg/min [16]; ~ 800 nmol dCDP/mg/min [35]) and the mouse R1 (130 nmol dCDP/mg/min [16]), suggesting low levels of active *S. pombe* R1 proteins in the preparation. Hence, the mechanistic basis for Spd1-mediated RNR inhibition remains to be elucidated.

In this study, we identified an *S. cerevisiae* gene encoding a protein with sequence homology to both Sml1 and Spd1. Since the submission of the manuscript, the same gene was named as *DIF1* (damage-regulated import factor) by an independent study because of its role in nuclear import of R2 and its regulation by the DNA damage checkpoint (27). *DIF1* orthologs are found in multiple fungal genomes. We demonstrate that Dif1 is required for proper nuclear localization of the R2 subunit. Dif1 is localized primarily in the cytoplasm and functions in a pathway separate from the Kap122-Wtm1 proteins. Blockage of nuclear export restores nuclear localization of R2 to the *wtm1Δ* but not the *wtm1Δ dif1Δ* cells. Dif1 is phosphorylated in response to DNA damage in a checkpoint kinase-dependent manner. Interestingly, phosphorylated Dif1 is enriched in the nucleus after DNA damage. We also show that regulation of Sml1 and Dif1 phosphorylation and proteolysis occurs through a homologous domain shared between the two proteins. Taken together, our results indicate that Dif1 plays

an important role in nuclear import of the R2 subunit and works concertedly with Kap122-Wtm1 to control the dynamic RNR subcellular localization in response to genotoxic stress.

MATERIALS AND METHODS

Strains, plasmids, and media. Strains and plasmids used in this study are listed in Table 1. Growth of yeast strains and genetic manipulations were performed as previously described (6). The complex medium YPD contained 1% Bacto yeast extract, 2% Bacto peptone, and 2% glucose. The synthetic complete medium contained 0.17% yeast nitrogen base without amino acids and (NH₄)₂SO₄ (MP Biomedicals), 0.5% (NH₄)₂SO₄, 2% glucose, and all 20 amino acids (Sigma) at concentrations as described previously (6). Selective (i.e., dropout) media were synthetic complete media omitting one or more amino acids. For solid media, 2% Bacto agar was added before autoclaving. G418 (Invitrogen) was used at 200 mg/liter; 5-fluoroorotic acid (5-FOA; Sigma) was used at 1 g/liter.

The *DIF1* open reading frame plus 459-bp 5' untranslated regions (UTRs) and a 193-bp 3' UTR was PCR amplified using wild-type yeast genomic DNA as a template and subcloned into pCR2.1-TOPO (Invitrogen) to generate pMH1487, which was used for subsequent subcloning and site-directed mutagenesis steps to generate *DIF1* constructs with desired mutations and deletions. All clones generated by PCR were confirmed by DNA sequencing.

Immunofluorescence microscopy and antibodies. Preparation of yeast spheroplasts, immunofluorescence staining, and image acquisition were performed as previously described (50). Polyclonal anti-Rnr1, anti-Rnr2, and anti-Rnr4 antibodies were described previously (50). Monoclonal anti-Myc (9E10) was purchased from Roche Applied Sciences, and polyclonal anti-Myc was from Santa Cruz Biotechnology. Horseradish peroxidase- and fluorescein isothiocyanate-conjugated goat anti-mouse and goat anti-rabbit antibodies were purchased from Jackson ImmunoResearch Labs. Polyclonal anti-Zwf1 (glucose-6-phosphate dehydrogenase) antibodies were purchased from Sigma, and monoclonal anti-Nop1 antibody was from EnCor Biotech.

Protein extraction, immunoblotting, and phosphatase treatment. Protein extracts were prepared by using glass bead disruption on a BeadBeater (BioSpec Products). Two different extraction solutions/buffers were used. For immunoblotting to detect steady-state levels of Dif1 protein, trichloroacetic acid was employed to extract protein from 1×10^7 to 1×10^8 mid-log-phase cells for each loading (2). For phosphatase treatment, protein extracts were prepared in buffer B (50 mM HEPES-KOH, pH 7.5, 140 mM NaCl, 1 mM EDTA, 1% Triton X-100, 0.1% sodium deoxycholate, 1 mM phenylmethylsulfonyl fluoride, supplemented with $1 \times$ protease inhibitor cocktail from Roche Applied Science) and centrifuged at $13,400 \times g$ for 15 min to remove debris. Protein concentrations were determined by using the Bradford protein assay (Bio-Rad). Twenty-five to 50 μ g of total protein extracts was incubated with 200 units lambda protein phosphatase (New England Biolabs) at 37°C for 30 min. A mixture of 0.1 mM Na₃VO₄ and 30 mM NaF was used as phosphatase inhibitor. Proteins were resolved by 8 to 12% sodium dodecyl sulfate-polyacrylamide gel electrophoresis (SDS-PAGE), transferred to nitrocellulose membranes, and probed with primary and secondary antibodies. Blots were developed with an enhanced chemiluminescence substrate (Perkin-Elmer).

Subcellular fractionation. Yeast cells (2×10^9) from mid-log-phase cultures were harvested, washed with and resuspended in 2 ml of preincubation buffer {100 mM PIPES [piperazine-N,N'-bis(2-ethanesulfonic acid)]-KOH at pH 9.4, 10 mM dithiothreitol (DTT)}, and incubated at 30°C for 10 min. Cells were then washed and resuspended in 4 ml of lysis buffer (50 mM Tris-HCl at pH 7.5, 10 mM MgCl₂, 1.2 M sorbitol, 1 mM DTT), and digested with 40 μ l of Zymolyase 200T (10 mg/ml) at 30°C until $>90\%$ of cells were lysed in fresh water (30 to 60 min). Cells were washed twice with lysis buffer and then resuspended in 4 ml of Ficoll buffer (18% [wt/vol] Ficoll-400, 10 mM Tris-Cl at pH 7.5, 20 mM KCl, 5 mM MgCl₂, 3 mM DTT, 1 mM EDTA, 1 mM phenylmethylsulfonyl fluoride, protease inhibitor cocktail; Roche) at 4°C. Cells were broken with 30 moderate to slow strokes in a Dounce homogenizer with a loose pestle. Unlysed cells were removed by spinning at $3,000 \times g$ for 15 min. The lysate was then spun at $20,000 \times g$ for 15 min. The resulting supernatant was labeled as cytosol, and the pellet was labeled as nuclei.

RESULTS

Identification of *DIF1*. By using position-specific iterative BLAST (PSI-BLAST) and pattern hit-initiated BLAST (PHI-BLAST) analyses with the *S. pombe* Spd1 protein and the *S.*

TABLE 1. Strains and plasmids used in this study

Strain or plasmid	Relevant genotype or description	Reference
Strains		
BY4741	<i>MATa his3Δ1 leu2Δ0 met15Δ0 ura3Δ0</i>	5
Y300	<i>MATa can1-100 ade2-1 his3-11,15 leu2-3,112 trp1-1 ura3-1 lys12</i>	1
Y582	<i>MATa mec1::HIS3 pBAD45 (CEN URA3 MEC1)</i>	18
MHY340	<i>MATα 3MYC-RNR2-kan</i>	This study
MHY363	<i>MATa sml1::kan</i>	50
MHY385	<i>MATα sml1::his5 mec1::HIS3</i>	50
MHY386	<i>MATa sml1::his5 mec1::HIS3 pBAD45 (CEN UAR3 MEC1)</i>	This study
MHY392	<i>MATα dun1::HIS3</i>	50
MHY497	<i>MATa kap122::kan</i>	51
MHY685	<i>MATa ade2-1 trp1-1 can1-100 leu2-3,112 his3-11,15 ura3 GAL⁺ psi⁺ wtm1::WTM1-18xMyc-TRP1</i>	51
MHY836	<i>MATα wtm1::kan</i>	51
MHY843	<i>MATa dif1::kan</i>	This study
MHY845	<i>MATa dif1::kan wtm1::kan</i>	This study
MHY847	<i>MATa dif1::kan kap122::kan</i>	This study
MHY849	<i>MATa dif1::kan sml1::his mec1::HIS3</i>	This study
MHY856	<i>MATα dif1::kan WTM1-18Myc-TRP1</i>	This study
MHY897	<i>MATa dif1::kan mec1::HIS3 pBAD4 (URA3 CEN MEC1)</i>	This study
XWY10	<i>MATa 3MYC-DIF1</i>	This study
XWY13	<i>MATa wtm1::kan crm1::kan pDC-CRM1(T539C)</i>	This study
XWY43	<i>MATa dif1::kan crm1::kan pDC-CRM1(T539C)</i>	This study
XWY15	<i>MATa wtm1::kan dif1::kan crm1::kan pDC-CRM1(T539C)</i>	This study
XWY23	<i>MATα dun1::HIS3 3MYC-DIF1</i>	This study
XWY24	<i>MATα sml1::his5 mec1::HIS3 3MYC-DIF1</i>	This study
MNY8	<i>MATa crm1::kan ade2 leu2 his3 trp1 ura3 pDC-CRM1(T539C)</i>	33
Plasmids		
pMH910	pRS414-SML1	This study
pMH914	pRS414-sml1(Δ28-50)	This study
pMH1487	pCR2.1TOPO-DIF1	This study
pMH1326	pRS416-GAL1-RNR4(1–340)-GFPsg-Tadh1	This study
pMH1489	pRS416-DIF1	This study
pMH1494	pRS314-P _{DIF1} -3MYC-DIF1	This study
pMH1546	pRS314-P _{TDH3} -3MYC-DIF1	This study
pXW15	pRS314-P _{DIF1} -3MYC-dif1(Δ79-103)	This study
pXW16	pRS314-P _{DIF1} -3MYC-dif1(T83A/S85A)	This study
pXW17	pRS314-P _{DIF1} -3MYC-dif1(T102A/S104A/T105A)	This study

cerevisiae Sml1 protein, we identified a hypothetical open reading frame in the *S. cerevisiae* genome, YLR437C. The predicted 133-residue polypeptide encoded by YLR437C shares sequence homology to Spd1 and Sml1, respectively. Thus, we originally named the open reading frame YLR437C as the *SDH1* gene (for Sml1 and Spd1 homology). Recently, the molecular characterization of this gene called *DIF1* has been reported (27). The N-terminal region of Dif1 (amino acids 22 to 57) is 33% identical and 47% similar to that of Spd1 (amino acids 16 to 51) (Fig. 1A and B), both of which are predicted to be of mostly alpha-helical secondary structure (Jpred 3, <http://www.compbio.dundee.ac.uk/~www-jpred/>). The C-terminal half of Dif1 (amino acids 76 to 114) is 43% identical and 57% similar to the central region of Sml1 (amino acids 25 to 66) (Fig. 1A and B). The homologous regions shared by Dif1 and Sml1 are relatively enriched in serine and threonine residues. It is worth noting that three serines within this region of Sml1 (S56, S58, and S60) were previously identified as being specifically phosphorylated by the Dun1 checkpoint kinase in vitro (45).

BLAST analysis revealed Dif1 orthologs and/or homologs among many species of the *Saccharomycetaceae* family; they are absent in other fungal species and higher eukaryotes. The

Spd1- and Sml1-homologous regions in Dif1 are highly conserved among its counterparts in the close relatives of *S. cerevisiae*, as well as among more distant relatives including *Ashbya gossypii*, *Kluyveromyces lactis*, and *Candida albicans* (Fig. 1C). Dif1 sequence similarities among the three distantly related species drop significantly outside the two conserved regions, suggesting that these regions may play an important functional role(s).

Roles of Dif1 in nuclear localization of the R2 subunit. To investigate the potential role of Dif1 in regulating RNR activity, we compared the subcellular localization patterns of the R2 subunit between the wild-type and *dif1Δ* mutant cells by indirect immunofluorescence. Nuclear localization of both Rnr2 and Rnr4, the two components of the heterodimeric R2 subunit, was deficient in *dif1Δ* cells. The majority of the mutant cells (>60% for Rnr2 and >80% for Rnr4) exhibited ubiquitous Rnr2 and Rnr4 signals in both the nucleus and the cytoplasm, in contrast to the predominantly nuclear localization pattern observed in the wild-type cells (Fig. 2A and B). The deficiency in nuclear localization of Rnr2 and Rnr4 in the *dif1Δ* mutant was rescued by introducing a copy of the wild-type *DIF1* gene on a centromeric plasmid (one to two copies per cell) (24), indicating that the R2 mislocalization phenotype is

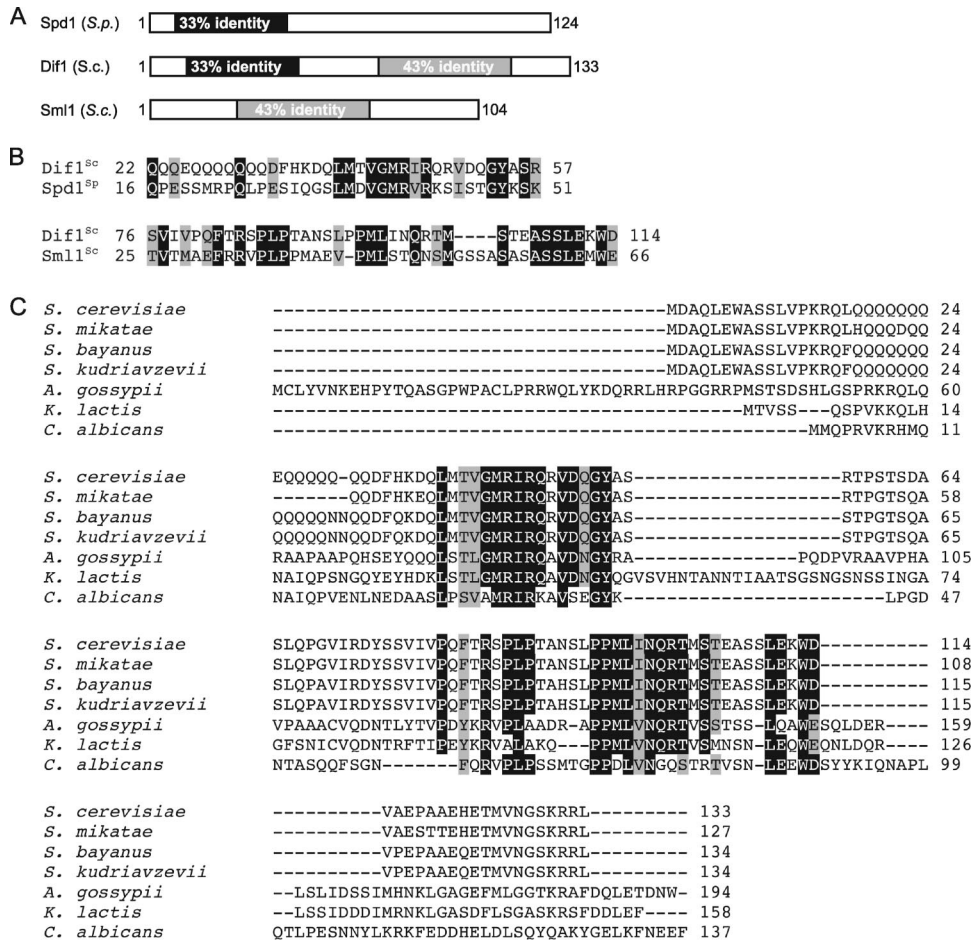


FIG. 1. Sequence alignment of Dif1^{Sc}, Sml1^{Sc}, Spd1^{Sp}, and other Dif1 orthologs. (A) Schematic representation of the homologous domain shared by Dif1^{Sc} and Spd1^{Sp} (in black) and that shared by Dif1^{Sc} and Sml1^{Sc} (in gray). Percentages of sequence identities are indicated. (B) Sequence alignment of residues 22 to 57 of Dif1^{Sc} with residues 16 to 51 of Spd1^{Sp} (top) and of residues 76 to 114 of Dif1^{Sc} with residues 25 to 66 of Sml1^{Sc} (bottom). Identical residues are shaded in black, and conserved residues are shaded in gray. (C) Alignment of the Dif1 orthologs from four *Saccharomyces* species (*S. cerevisiae*, *S. mikatae*, *S. bayanus*, and *S. kudriavzevii*) and *Ashbya gossypii*, *Kluyveromyces lactis*, and *Candida albicans*. Identical residues are shaded in black, and conserved residues are shaded in gray.

attributable to the absence of *DIF1* (Fig. 2B). The loss of R2 nuclear localization in the *dif1Δ* mutant is unlikely a cell cycle artifact, as *dif1Δ* cells showed similar defects when examined in log phase or G₁ and G₂/M phase of the cell cycle (Fig. 2A).

The karyopherin protein Kap122 and WD40 repeat protein Wtm1 have previously been shown to be required for proper nuclear localization of the R2 subunit (26, 51). The two proteins act in the same pathway, as the R2 mislocalization phenotype does not differ between the *kap122Δ wtm1Δ* double mutant and each single mutant (51). Kap122 interacts with Wtm1 in vivo and is required for nuclear localization of Wtm1 (51). To determine whether Dif1 functions in the same pathway as Kap122 and Wtm1 in controlling R2 localization, we constructed *dif1Δ kap122Δ* and *dif1Δ wtm1Δ* mutants and compared Rnr4 localization patterns of the double mutants to those of the *dif1Δ*, *kap122Δ*, and *wtm1Δ* single mutants. The mislocalization phenotype of Rnr4 was more severe in the double mutants than in each single mutant. While the single mutants exhibited predominantly a ubiquitous localization pattern characterized by Rnr4 signals equal between the nucleus

and cytoplasm, the double mutants displayed a predominantly cytoplasmic Rnr4 localization pattern (Fig. 2C). We conclude that Dif1 functions in a pathway that is separate from Kap122 and Wtm1. Consistent with this notion, we found that, unlike *KAP122*, *DIF1* is not required for the nuclear localization of Wtm1 or its close sequence homolog Wtm2, also a nuclear protein (Fig. 2D).

Dif1 is primarily localized in the cytoplasm and at substoichiometric levels relative to the R2 subunit. We posited that Dif1 could be involved in nuclear import of the R2 subunit or in retaining R2 in the nucleus. Previous studies showed that the nuclear protein Wtm1 functions to anchor R2 in the nucleus (26) and that Kap122 is required for importing Wtm1 into the nucleus (51). The finding that Dif1 acts in a pathway different from that of Wtm1 and Kap122 argues against a nuclear anchor role for Dif1. To further distinguish between the two possibilities, we examined Dif1 subcellular localization by inserting an N-terminal 3MYC epitope between the 5' UTR and the coding sequence of *DIF1* in its own chromosomal locus and monitoring Myc^{Dif1} in different subcellular fractions by

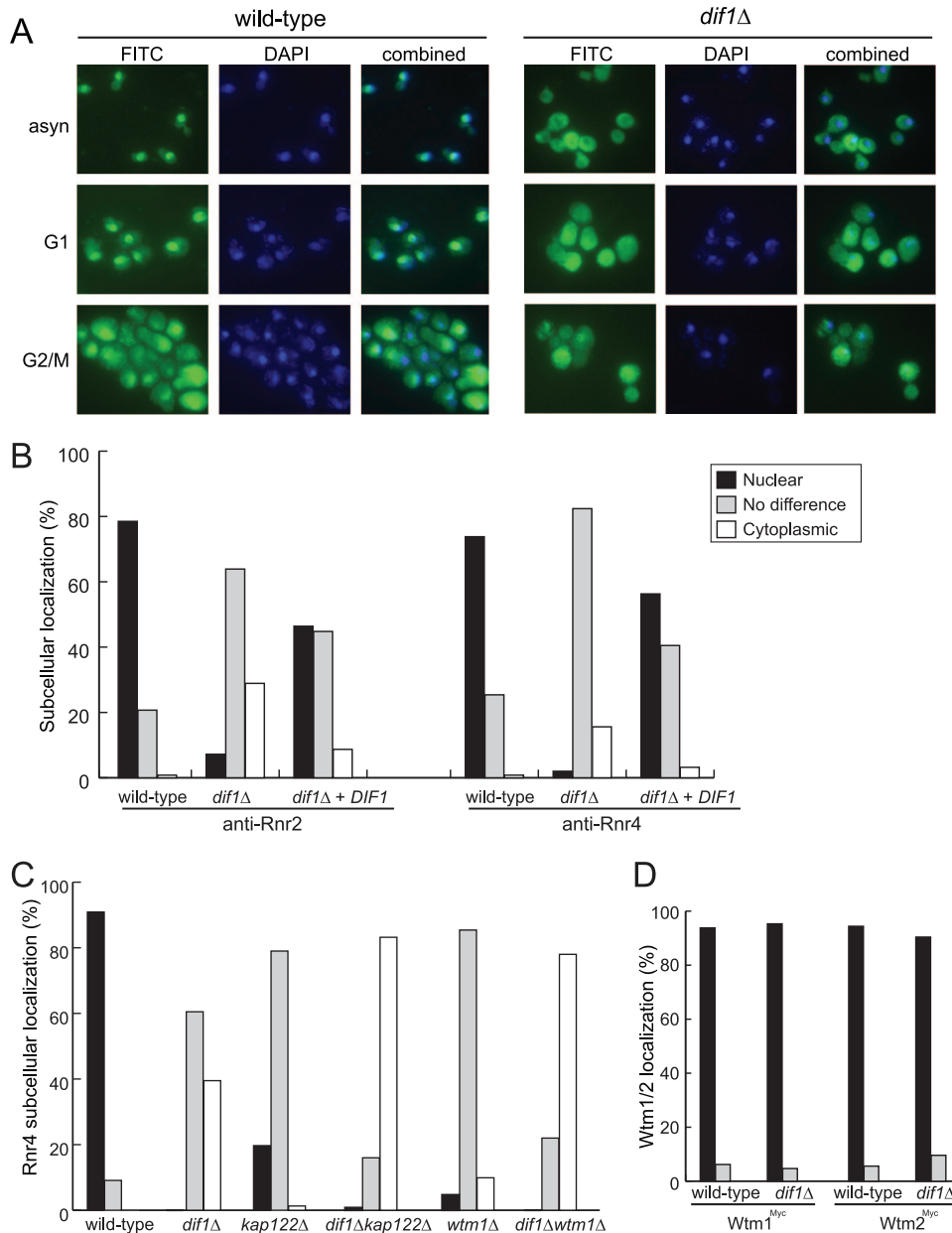


FIG. 2. Dif1 is required for proper nuclear localization of R2 and acts in a different pathway from Kap122 and Wtm1. (A) Wild-type (left panel) and *dif1Δ* (right panel) cells from asynchronous (asyn), α -factor-arrested G_1 -phase, and nocodazole-arrested G_2/M -phase cultures were stained with 4',6-diamidino-2-phenylindole (DAPI) for DNA and anti-Rnr2 antibodies for indirect immunofluorescence. FITC, fluorescein isothiocyanate. (B to D) Quantitative analyses of Rnr2 and/or Rnr4 subcellular localization by indirect immunofluorescence. For each experiment, >150 cells were counted for each strain. The indirect immunofluorescence analyses were repeated two to three times, and a representative result is shown. Percentages of cells with distinct localization patterns are represented as follows: black bars, cells with a predominantly nuclear signal; white bars, cells with a predominantly cytoplasmic signal; gray bars, cells with no difference in signal intensities between the nucleus and the cytoplasm. (B) Comparison of subcellular localization patterns of Rnr2 and Rnr4 in the wild-type, *dif1Δ*, and *dif1Δ* cells harboring a copy of wild-type *DIF1* on a centromeric plasmid (one to two copies/cell) (24). (C) Comparison of Rnr4 subcellular localization patterns in *dif1Δ*, *kap122Δ*, and *wtm1Δ* single mutants and *dif1Δ kap122Δ* and *dif1Δ wtm1Δ* double mutants. (D) Subcellular localization of Wtm1 and Wtm2 in the wild-type and *dif1Δ* cells.

Western blotting. Cells harboring ^{MYC}DIF1 at its endogenous chromosomal locus exhibited no difference in R2 subcellular localization pattern or sensitivity to DNA-damaging reagents relative to the wild-type cells (data not shown), indicating that ^{MYC}Dif1 functions normally as the native protein. Protein blotting of subcellular fractionation revealed that ^{MYC}Dif1 is pri-

marily in the cytoplasmic fraction (Fig. 3A), consistent with a role of importing the R2 subunit into the nucleus. The integrity of the subcellular fractionation was confirmed by blotting for the nucleolar protein Nop1 (39) and the cytoplasmic glucose-6-phosphate dehydrogenase Zwf1 (19) (Fig. 3A).

We compared the endogenous protein levels of Dif1 and the

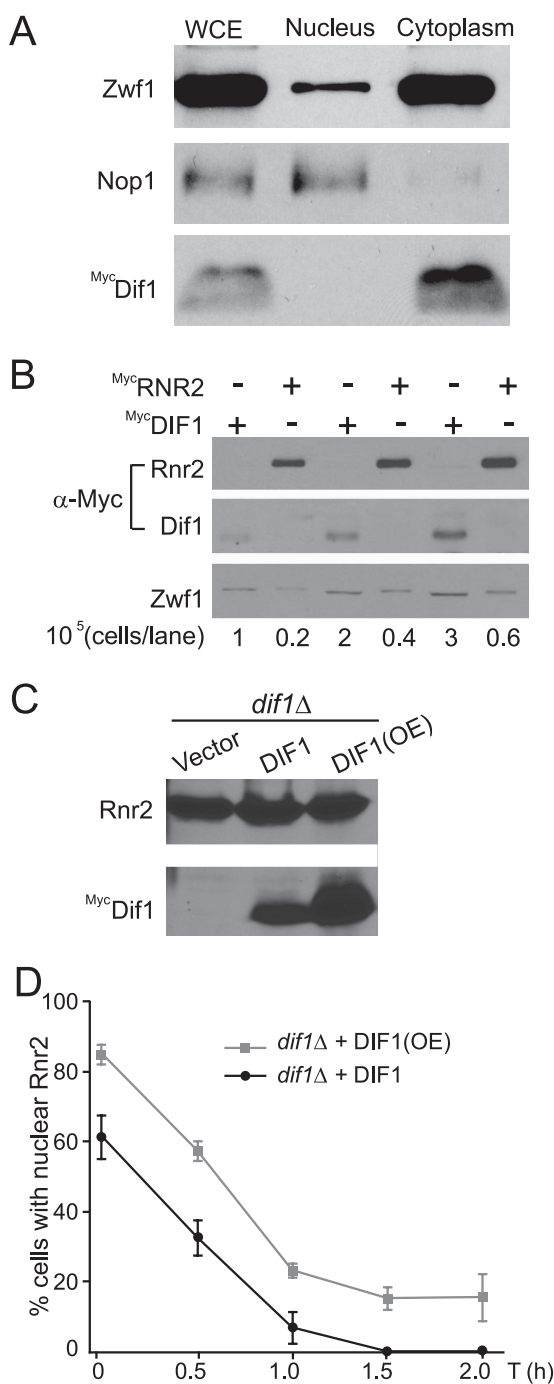


FIG. 3. Cytoplasmic localization of Dif1 and delay of DNA damage-induced R2 redistribution by Dif1 overexpression. (A) Dif1 is primarily localized in the cytoplasm. Log-phase wild-type cells containing an integrated copy of ^{MYC}DIF1 in the chromosomal DIF1 locus were fractionated into different subcellular compartments. Proteins extracted from whole-cell (WCE), cytoplasmic, and nuclear fractions were resolved by 12% SDS-PAGE and blotted with anti-Myc (^{MYC}Dif1), anti-NOP1 (a nucleolar protein), and anti-Zwf1 (glucose-6-phosphate dehydrogenase [G6DPH], a cytoplasmic protein). (B) Comparison of endogenous Dif1 and Rnr2 protein levels. Protein extracts from cells (cell numbers as indicated) containing N-terminally 3MYC-tagged DIF1 or RNR2 at its respective chromosomal locus were resolved on 12% SDS-PAGE and blotted with a monoclonal anti-Myc antibody and anti-Zwf1 antibodies (G6DPH) as a loading control. The chemiluminescence exposure times for ^{MYC}Dif1 and ^{MYC}Rnr2 were 1 min

R2 subunit by blotting for the Myc epitope in two integrated strains bearing N-terminal 3MYC-tagged Dif1 and Rnr2, respectively. Like ^{MYC}DIF1, ^{MYC}RNR2 was integrated in the chromosomal RNR2 locus under the control of the native RNR2 promoter. Cells containing ^{MYC}RNR2 exhibited no difference from the wild-type cells in growth rate or sensitivity to hydroxyurea (HU) (data not shown), a free radical scavenger that inhibits the R2 subunit. Indirect immunofluorescence analyses showed that ^{MYC}Rnr2 is predominantly localized in the nucleus under normal growth conditions and undergoes nucleus-to-cytoplasm redistribution in response to genotoxic stress like the native Rnr2 does (data not shown). Taken together, these data suggest that ^{MYC}Rnr2 functions similarly to the native Rnr2 protein and that the ^{MYC}Rnr2 protein levels reflect the endogenous Rnr2 levels. Blotting with anti-Myc antibodies revealed that the static protein level of ^{MYC}Dif1 is >10-fold lower than that of ^{MYC}Rnr2 (Fig. 3B). Thus, Dif1 is present at substoichiometric levels relative to the R2 subunit, both of them being primarily in the cytoplasm.

Dif1 overexpression results in an increase in R2 nuclear localization even in the presence of DNA damage. While introducing DIF1 on a centromeric plasmid (one to two copies per cell) (24) into the *dif1Δ* mutant cells restored the predominantly nuclear localization pattern of the R2 subunit, overexpression of DIF1 from the stronger and constitutively active TDH3 promoter (Fig. 3C) (3) led to an increase in R2 nuclear localization both in cells under normal growth conditions and in cells treated with the DNA-damaging reagent methyl methanesulfonate (MMS) (Fig. 3D). With the native DIF1 promoter, the percentages of cells exhibiting a predominantly nuclear Rnr2 signal decreased from 60% to <10% within 1 h of MMS treatment. In contrast, cells expressing DIF1 from the TDH3 promoter showed a higher Rnr2 nuclear signal (80% versus 60%) at time zero and maintained a higher R2 nuclear localization throughout the time course of MMS treatment, with a plateau at 20% even after 2 h in MMS (Fig. 3D). Interestingly, cells expressing different levels of Dif1 exhibited a similar decline in the nuclear presence of R2 (Fig. 3D). The observed delay in R2 redistribution is not due to any fluctuation in R2 protein abundance, as the Rnr2 protein levels remained the same in cells containing no DIF1 or one copy of

and 5 s, respectively. The slight difference in migration positions of Zwf1 is likely attributable to unequal loading of the two protein extracts in neighboring lanes (cell numbers per lane as indicated). (C) Dif1 overexpression does not affect endogenous Rnr2 protein levels. Protein extracts from *dif1Δ* cells harboring a centromeric plasmid (one to two copies/cell) (24) that expressed an N-terminally 3MYC-tagged DIF1 from the native DIF1 promoter or the constitutive TDH3 promoter (OE) were resolved on 12% SDS-PAGE and blotted with anti-Rnr2 and anti-Myc antibodies. (D) Dif1 overexpression delays MMS-induced Rnr2 redistribution from the nucleus to the cytoplasm. Log-phase *dif1Δ* cells harboring a centromeric plasmid expressing N-terminally 3MYC-tagged DIF1 from the native DIF1 promoter (*dif1Δ* + DIF1) or the constitutive TDH3 promoter [*dif1Δ* + DIF1(OE)] were treated with 0.03% MMS and collected at the indicated time points for indirect immunofluorescence with anti-Rnr2 antibodies. Three independent clones were processed for immunofluorescence, with >150 cells examined for each time point. Shown are percentages of cells with a predominantly nuclear signal. The error bars represent standard deviations.

DIF1 under its endogenous promoter or *DIF1* under the *TDH3* promoter (Fig. 3C).

Inhibition of Crm1-mediated nuclear export restores nuclear localization of R2 to the *wtm1Δ* cells but not the *dif1Δ* and *wtm1Δ dif1Δ* cells. The dynamic change in subcellular localization patterns of the R2 subunit during the mitotic cell cycle and in response to DNA damage could result from changes in either nuclear import or nuclear export of R2 or a combination of both. To investigate the role of nuclear export in modulating R2 localization, we utilized the *crm1(T539C)* strain that is sensitive to the exportin inhibitor leptomycin B (33) and a *GAL1* promoter-controlled Rnr4-green fluorescent protein (GFP). Synthesis of the Rnr4-GFP fusion protein was induced for 90 min and terminated by change of carbon source. Two hours after promoter shutoff, the Rnr4-GFP is primarily found in the nucleus in both the wild-type (*CRM1*) and *crm1(T539C)* cells (Fig. 4A, time zero). MMS treatment resulted in rapid decrease in nuclear Rnr4-GFP signals in both the wild-type (*CRM1*) and *crm1(T539C)* cells, indicating that the *crm1(T539C)* allele does not affect R2 localization or damage-induced redistribution in the absence of leptomycin B. Leptomycin B treatment alone exhibited no effect on nuclear Rnr4-GFP signals in the wild-type (*CRM1*) cells. A transient decrease in nuclear Rnr4-GFP signals was observed in the *crm1(T539C)* cells after leptomycin B treatment (at the 1-h point), but these signals recovered to the wild-type levels at later time points (Fig. 4A, right panel). As anticipated, MMS treatment led to a steady decline of nuclear Rnr4-GFP in both the *CRM1* and *crm1(T539C)* cells, correlating with redistribution of R2 from the nucleus to the cytoplasm. Addition of leptomycin B to the MMS-treated *CRM1* cells did not prevent the loss of nuclear Rnr4-GFP (Fig. 4A, left panel). In contrast, addition of leptomycin B to the MMS-treated *crm1(T539C)* cells resulted in retention of nuclear Rnr4-GFP in 40% of the cells up to the 3-h point (Fig. 4A, right panel). The data suggest that in addition to nuclear import and nuclear anchoring, nuclear export also contributes to the dynamic changes in subcellular localization of the R2 subunit.

We then wanted to determine whether blocking Crm1-mediated nuclear export can reverse the deficiency of R2 nuclear localization in cells lacking Wtm1 and Dif1 in the leptomycin B-sensitive *crm1(T539C)* background. Leptomycin B restored nuclear localization of R2 to the majority of the *wtm1Δ* cells, from 10% to 70% (Fig. 4B), suggesting that blocking of nuclear export can compensate for loss of nuclear anchoring of R2 in the absence of Wtm1. Conversely, leptomycin B failed to restore nuclear localization of R2 in either the *dif1Δ* cells or the *wtm1Δ dif1Δ* cells (Fig. 4B); the majority of the double mutant cells (>90%) exhibited a ubiquitous R2 signal in both the nucleus and the cytoplasm in the presence of leptomycin B (Fig. 4B). We also showed that leptomycin B treatment did not change the subcellular distribution of Dif1, which remained in the cytoplasm (Fig. 4C). These results are consistent with a model in which Dif1 is required for nuclear import rather than nuclear anchoring of the R2 subunit.

Checkpoint-dependent phosphorylation of Dif1 and diminution of Dif1 protein levels in response to genotoxic stress. In response to DNA damage and replication blockage, the R2 subunit undergoes nucleus-to-cytoplasm redistribution in a checkpoint-dependent manner (50). To investigate how Dif1

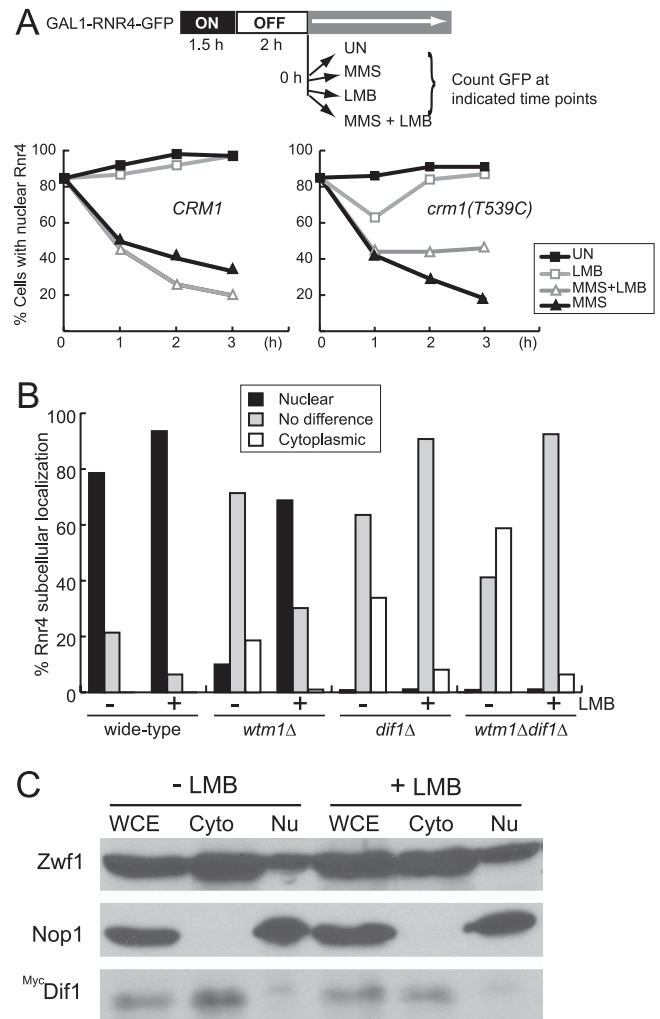


FIG. 4. Inhibition of Crm1-dependent nuclear export restores nuclear localization of R2 to the *wtm1Δ* but not *wtm1Δ dif1Δ* cells. (A) MMS-induced nucleus-to-cytoplasm redistribution of Rnr4-GFP is partially dependent on Crm1-mediated nuclear export. Wild-type (*CRM1*) and leptomycin B (LMB)-sensitive mutant [*crm1(T539C)*] cells, both harboring the *GAL1-RNR4-GFP* plasmid, were grown in raffinose to log phase. Expression of Rnr4-GFP was induced by addition of 2% galactose to the medium and turned off 90 min later by addition of 2% glucose. At 2 h after promoter shutoff ($t = 0$ h), the culture was split into four parts: one was left untreated (UN), and the other three were treated with 0.025% MMS, 50 ng/ml of LMB, or 50 ng/ml LMB in combination with 0.025% MMS (MMS + LMB), respectively. Subcellular localization of Rnr4-GFP was visualized in live cells, and the percentage of cells containing a predominantly nuclear GFP signal was presented. The time course experiment was repeated three times; shown is a representative result. (B) All four strains are in the LMB-sensitive *crm1(T539C)* background. Wild-type, *wtm1Δ*, *dif1Δ*, and *wtm1Δ dif1Δ* cells were grown to log phase and split into two parts: one was untreated, and the other was incubated with 100 ng/ml of LMB in the medium for 45 min before being processed for indirect immunofluorescence with anti-Rnr4 antibodies. Quantitative analysis of subcellular localization patterns and bar shading are the same as in Fig. 2. (C) Log-phase *crm1(T539C)* cells expressing N-terminally 3MYC-tagged *DIF1* from its native promoter were untreated or incubated with 100 ng/ml of LMB for 45 min before being processed for subcellular fractionation. Protein extracts of the whole-cell (WCE), cytoplasmic (Cyto), and nuclear (Nu) fractions were resolved by 12% SDS-PAGE and blotted with anti-Myc, anti-Nop1, and anti-Zwf1 antibodies as described in the legend to Fig. 3A.

might contribute to the dynamic changes in R2 localization, we examined the ^{Myc}Dif1 protein levels in cells being treated with MMS and HU. As shown in Fig. 5A, the levels of the ^{Myc}Dif1 protein decreased gradually after MMS treatment. The MMS-induced decrease in ^{Myc}Dif1 protein levels is likely attributable to posttranscriptional regulation because *DIF1* transcript levels do not change after MMS treatment (15). Moreover, slower-migrating species of ^{Myc}Dif1 were observed in MMS-treated cells from as early as the 15-min point, accompanying the disappearance of the protein. Similarly, slower-migrating forms of ^{Myc}Dif1 and a decrease in ^{Myc}Dif1 protein levels were also observed in cells being treated with HU (Fig. 5B). The change in ^{Myc}Dif1 mobility results from protein phosphorylation, because it was reversed by phosphatase treatment and this conversion was blocked by the addition of phosphatase inhibitors (Fig. 5C). The phosphorylated form of ^{Myc}Dif1 was undetected and/or greatly diminished in the *mec1Δ* and *dun1Δ* mutants after HU and MMS treatment, indicating that Dif1 phosphorylation is dependent on the DNA damage checkpoint kinases Mec1 and Dun1. The residual Dif1 phosphorylation in MMS-treated *mec1Δ* cells is likely due to partially redundant DNA damage signaling through the Mec1 homology Tel1 kinase (11, 38). Interestingly, we observed accumulation of phosphorylated forms of the ^{Myc}Dif1 protein inside the nucleus after cells were treated with HU and MMS (Fig. 5E and F), suggesting that phosphorylation and subsequent degradation of the protein take place in the nucleus.

A conserved domain is involved in controlling protein stabilities of Sml1 and Dif1. To identify which region in Dif1 is involved in checkpoint kinase-mediated phosphorylation of the protein in response to DNA damage, we examined sequence alignment between Dif1 and Sml1. Like Dif1, the Sml1 protein undergoes checkpoint kinase-dependent phosphorylation and diminishes significantly in cells treated with MMS and HU (52, 55). The Dun1 kinase has been shown to be directly required for Sml1 phosphorylation in vivo (55). Previous biochemical studies have identified three serines (S60, S56, and S58) in the middle region of Sml1 that are phosphorylated by Dun1 (45), although their physiological significance in controlling Sml1 phosphorylation and protein stability is not known. The three serine residues reside at the C-terminal half of the homologous region shared by Sml1 and Dif1 (Fig. 1A and B). Residues 28 to 50 of Sml1 were predicted to be a nonstructural linker region between the N- and C-terminal alpha-helical regions of the protein; removal of this region does not affect Sml1's inhibition of RNR activity (53). We found that removal of residues 28 to 50 in Sml1 greatly increased stability of the protein both in cells under normal growth conditions and in cells treated with HU and MMS (Fig. 6A). Consistent with previous reports, a slower-migrating form(s) of the full-length Sml1 was observed in cells treated with HU and MMS (Fig. 6A), indicative of Sml1 phosphorylation (52, 55). In contrast, no change in mobility of Sml1(Δ28–50) was observed after HU and MMS treatment. We therefore conclude that residues 28 to 50 of Sml1 constitute a subdomain responsible for the phosphorylation and degradation of the protein. Interestingly, removal of the corresponding region in Dif1 (residues 79 to 103) also abolished the MMS-induced, lower-mobility form of Dif1 and enhanced Dif1 protein stability after MMS treatment relative to the full-length Dif1 (Fig. 6B). There are five serine/threo-

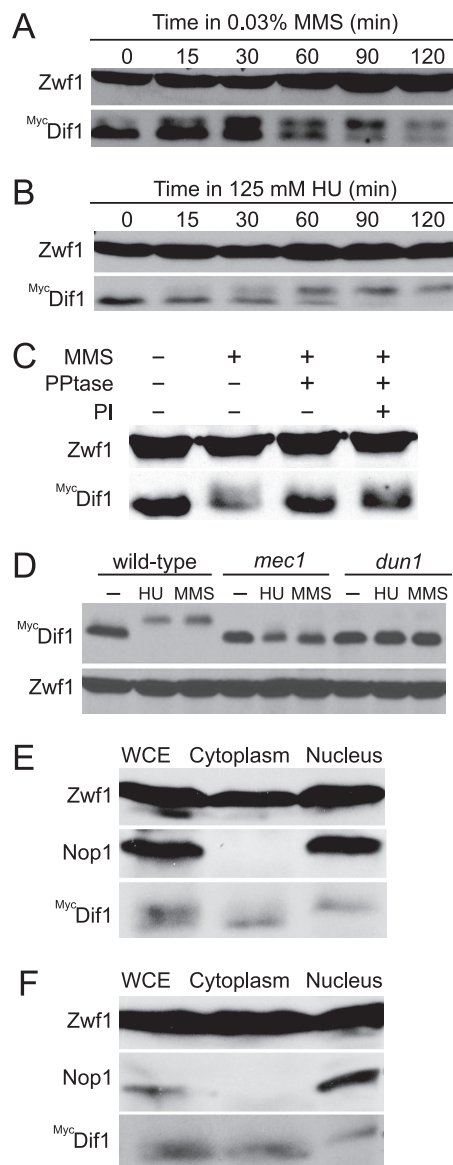


FIG. 5. Genotoxic stress-induced phosphorylation of Dif1 and decrease in Dif1 protein levels depend on the checkpoint kinases Mec1 and Dun1. All strains used here contain an integrated copy of ^{Myc}*DIF1* in the chromosomal *DIF1* locus. (A and B) Log-phase wild-type cells were incubated with 0.03% MMS (A) or 125 mM of HU (B) and harvested at the indicated time points. Protein extracts were made, resolved by 12% SDS-PAGE, and probed with anti-^{Myc}Dif1 and anti-Zwf1 (glucose-6-phosphate dehydrogenase [G6DPH]) as a loading control. (C) Protein extracts from the 0- and 120-min points in panel A were incubated with lambda phosphatase (PPTase) at 37°C for 30 min, with and without phosphatase inhibitors (PI) Na₃VO₄ and NaF. ^{Myc}Dif1 and anti-Zwf1 were probed on a protein blot as described for panel A. (D) Log-phase wild-type, *mec1Δ* *sml1Δ*, and *dun1Δ* cells were kept untreated or treated with 125 mM of HU and 0.03% MMS for 2 h before being harvested for protein extraction. ^{Myc}Dif1 and anti-Zwf1 were probed on a protein blot as described for panel A. (E and F) Detection of phosphorylated ^{Myc}Dif1 in the nucleus fraction after MMS and HU treatment. Wild-type cells were incubated with 0.03% MMS (E) and 125 mM HU (F) for 1 h and fractionated to different subcellular compartments. Probing of ^{Myc}Dif1, Nop1, and Zwf1 (G6DPH) was performed as described in the legend to Fig. 3A.

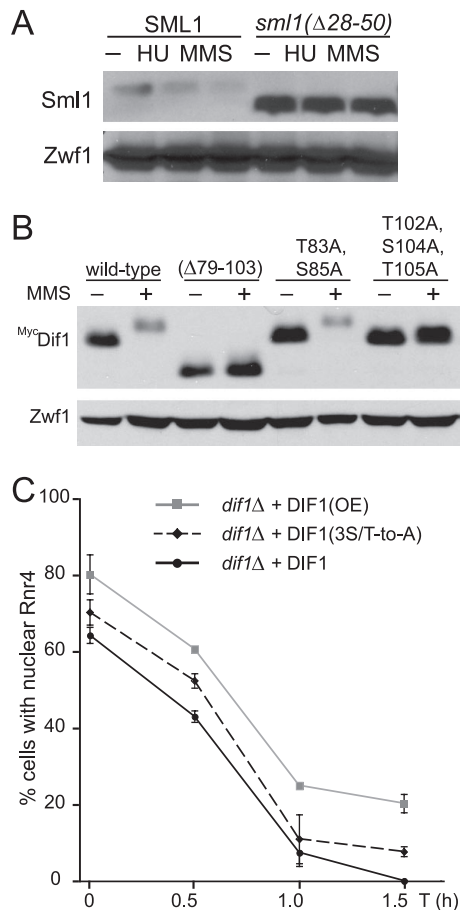


FIG. 6. A common domain shared by Sml1 and Dif1 controls Dif1 phosphorylation and protein stability in response to DNA damage. (A) Residues 28 to 50 of Sml1 control its protein stability. Protein extracts of log-phase wild-type (*SML1*) and *sml1*($\Delta 28-50$) cells, untreated or after treatment with 125 mM of HU and 0.03% MMS for 2 h, were probed with anti-Sml1 and anti-Zwf1 antibodies as a loading control on a protein blot. (B) All strains shown are *dif1* Δ strains that contain various N-terminally 3MYC-tagged *DIF1* alleles under the *DIF1* promoter on a centromeric plasmid. Log-phase cultures were untreated or incubated with 0.03% MMS for 2 h, and protein extracts were made and probed with anti-Myc and anti-Zwf1 antibodies as a loading control on a protein blot. The $\Delta 79-103$ construct contains a deletion of residues 79 to 103; the T83A, S85A construct contains alanine substitutions at T83 and S85; the T102A, S104A, T105A construct contains alanine substitutions at T102, S104, and T105. (C) Delay in MMS-induced nucleus-to-cytoplasm redistribution of Rnr4 in a phosphorylation-deficient mutant of the *DIF1* strain. Log-phase *dif1* Δ cells containing a centromeric plasmid that expresses the wild-type *DIF1* from the *DIF1* promoter (*dif1* Δ + DIF1, solid black line) or from the constitutive *TDH3* promoter [*dif1* Δ + DIF1(OE), gray line] and the phosphorylation-deficient T102A/S104A/T105A mutant from the *DIF1* promoter [*dif1* Δ + DIF1(3S/T-toA), dashed black line] were treated with 0.03% MMS and harvested at the indicated time points for indirect immunofluorescence with anti-Rnr4 antibodies. Quantitative analysis of Rnr4 subcellular localization and data presentation were performed as described in the legend to Fig. 3D.

nine residues between residues 79 and 103 of Dif1, although only T102 is conserved between Dif1 and Sml1. In addition, the adjacent residue S104 corresponds to S56 in Sml1, which was one of the three Dun1 phosphorylation sites identified *in vitro*. We made S/T-to-A alterations in all five S/T residues within

the region 79 to 103, as well as in S104 and its neighboring T105, individually and in combination, and determined their effects on Dif1 phosphorylation and protein stability after MMS treatment. Of all the mutants, only the triple substitution T102A/S104A/T105A drastically decreased Dif1 phosphorylation and increased its stability (Fig. 6B). We conclude that the three residues T102/S104/T105 are the major sites for controlling DNA damage-induced phosphorylation and degradation of the Dif1 protein.

To understand the biological significance of change in Dif1 phosphorylation and stability in response to DNA damage, we compared MMS-induced R2 redistribution between the wild-type cells and cells harboring the *dif1*(T102A/S104A/T105A, i.e., 3S/T-to-A) mutant allele. The *dif1*(3S/T-to-A) mutant exhibited a moderate but reproducible increase in Rnr4 nuclear localization throughout the time course of MMS treatment relative to the wild-type strain (Fig. 6C). The fraction of the *dif1*(3S/T-to-A) mutant cells maintaining a predominantly nuclear R2 signal is between that of the *dif1* Δ cells expressing physiological levels of Dif1 from the native promoter and that of the cells overexpressing Dif1 from the constitutive *TDH3* promoter (Fig. 6C). Thus, removal of the three phosphorylation sites stabilizes Dif1 in cells experiencing DNA damage, leading to a decrease in the redistribution of R2 from the nucleus to the cytoplasm.

Deletion of *DIF1* suppresses *mec1* Δ lethality and enhances HU resistance of *mec1* Δ *sml1* Δ cells. It has been shown elsewhere that changes in the RNR holoenzyme levels and activities can affect cellular resistance to the RNR inhibitor HU, as well as viability of the *mec1* Δ checkpoint mutant (13, 26, 54). Deletion of the R1 inhibitor *SML1* and overexpression of R1 both suppress the lethality of *mec1* Δ , indicating that increased RNR activity can bypass the essential function of *MEC1* (13, 54). Because cytoplasmic colocalization of the R2 and R1 subunit in the *dif1* Δ mutant increases the chance of RNR holoenzyme formation, we wanted to determine if *dif1* Δ can also bypass the essential function of *MEC1*. As shown in Fig. 7A, *dif1* Δ does suppress the lethality of *mec1* Δ , although to a lesser degree relative to *sml1* Δ . Removal of *DIF1* also increased cellular resistance to HU in the *mec1* Δ *sml1* Δ background (Fig. 7B). The increased HU resistance conferred by *dif1* Δ does not result from an increase in protein levels of the two RNR subunits, as Rnr1 and Rnr4 protein levels remained the same between the *mec1* Δ *sml1* Δ and *mec1* Δ *sml1* Δ *dif1* Δ cells (Fig. 7C).

DISCUSSION

Maintaining proper dNTP pool sizes and relative ratios among the four dNTPs is critical for faithful DNA replication and repair, thereby directly impacting genomic integrity and cell survival. Cells exert control of the dNTP pools by regulating the RNR enzyme that is essential to supply the majority of the building blocks for DNA synthesis in all organisms. The RNR levels and activities are thus modulated both during normal cell cycle progression in proliferating cells and in response to genotoxic stress in all cells, to ensure that dNTPs are made when needed and in the right amount (34). With the exception of regulation by allosteric effectors, all three major regulatory pathways of RNR, namely, transcription, inhibitor

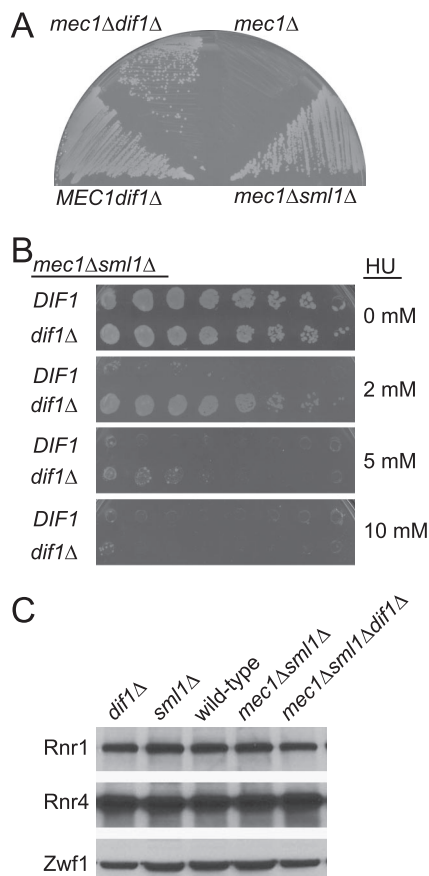


FIG. 7. Deletion of *DIF1* suppresses *mec1Δ* lethality and increases HU resistance of the *mec1Δ sml1Δ* cells. (A) The *mec1Δ*, *mec1Δ sml1Δ*, and *mec1Δ dif1Δ* cells, all harboring a *CEN6 URA3 MEC1* plasmid, were grown on a 5-FOA plate for 3 days at 30°C. Growth on the 5-FOA plate indicates survival of *mec1Δ* cells in the absence of the wild-type *MEC1* on the *URA3* plasmid. The *dif1Δ* single mutant (*MEC1 dif1Δ*) is shown as a control. (B) Serial 10-fold dilutions of the *mec1Δ sml1Δ* and *mec1Δ sml1Δ dif1Δ* cells were spotted on YPD plates containing increasing concentrations of HU and grown for 2 days at 30°C. (C) Protein extracts of log-phase cells of the indicated strains were probed with anti-Rnr1, anti-Rnr4, and anti-Zwf1 antibodies as a loading control.

stability, and subcellular localization, are controlled by the cell cycle and DNA damage checkpoint kinases. Several recent studies have highlighted the importance of dynamic subcellular localization patterns of the R2 subunit in regulating RNR activity (26, 29, 30, 50). This study provides new insights into the mechanism of R2 nuclear localization.

***dif1* in nuclear import of the R2 subunit.** In both fission yeast and budding yeast, the R2 subunit is primarily localized in the nucleus except for S phase of the cell cycle. In cells encountering DNA damage or replication blockage, R2 becomes redistributed from the nucleus to the cytoplasm and colocalized with the constitutively cytoplasmic R1 subunit in order to increase RNR holoenzyme formation (29, 50). The key player in controlling *S. pombe* R2 nuclear localization is Spd1, which anchors R2 in the nucleus and is targeted to degradation by the Cop9/signalosome in response to genotoxic stress (4, 29, 43). In *S. cerevisiae*, the WD40 repeat protein Wtm1 acts as a nuclear anchor of R2 (26, 51). However, neither the Wtm1 protein

level nor its nuclear localization is affected by DNA damage or replication blockage (26, 51), raising the question of what accounts for the decline of nuclear R2 levels in cells under genotoxic stress.

We have identified *S. cerevisiae* Dif1 based on its limited sequence homology to *S. pombe* Spd1, as well as *S. cerevisiae* Sml1, an inhibitor of the R1 subunit (54). Initial analysis revealed that Dif1 is required for nuclear localization of R2, adding a new player in the control of R2 localization. Several lines of evidence support a model in which Dif1 is directly involved in importing R2 into the nucleus. We have demonstrated that Dif1 functions in a separate pathway from Wtm1 and its nuclear importin Kap122 in controlling R2 nuclear localization. Moreover, the Dif1 protein is primarily localized in the cytoplasm, thus excluding the possibility of its being a nuclear anchor of R2. We have also shown that the endogenous protein level of Dif1 is >10-fold lower than that of R2, making it unlikely to form a stoichiometric protein complex with R2 to keep it in the nucleus. More importantly, we have shown that inhibition of Crm1-mediated nuclear export can partially restore nuclear localization of R2 in the *wtm1Δ* cells but not the *wtm1Δ dif1Δ* cells. Thus, it would appear that the nuclear R2 levels of R2 are a net result of nuclear import by Dif1, nuclear retention by Wtm1, and nuclear export via Crm1. In *wtm1Δ* cells, blockage of Crm1-mediated export by leptomycin B can partially compensate for the loss of nuclear anchoring, as Dif1 keeps importing R2 into the nucleus. Leptomycin B is no longer effective in *wtm1Δ dif1Δ* cells because of the absence of both nuclear import and nuclear retention.

How does Dif1 facilitate nuclear import of R2? An intriguing possibility is that the conserved N-terminal region in both Dif1 and Spd1 is involved in interaction with R2. The missing supporting evidence for a direct role of Dif1 in transporting R2 is protein-protein interaction between the two molecules. We have attempted to detect Dif1-R2 interaction under physiological levels of the two proteins in vivo by coimmunoprecipitation, but without success. This is likely due to the low static protein level of Dif1 and/or the transient nature of the Dif1-R2 interaction. It is also possible that epitope tagging of Dif1 impedes its interaction with R2. Nevertheless, we have tested both N-terminal 3MYC and C-terminal 3HA tagging of Dif1. Both the tagged proteins restored the nuclear localization and MMS-induced redistribution of R2 to the *dif1Δ* cells, but we were unable to detect their physical interaction with R2 by coimmunoprecipitation.

A common mechanism controlling Sml1 and Dif1 degradation. The sequence homology between Dif1 and Sml1 raises the question of whether Dif1 functions like Sml1 in binding and inhibiting the R1 subunit. This is unlikely to be the case because the shared region in Sml1 is dispensable for R1 binding and inhibition (53). Our finding that deletion of *DIF1* increases HU resistance of the *mec1Δ sml1Δ* cells also supports the notion that Dif1 and Sml1 inhibit RNR activity via different mechanisms.

The region shared by Dif1 and Sml1 is characterized by a high content of serine and threonine residues. Previous studies have identified three major phosphorylation sites within this region (S56, D58, and S60) by the Dun1 kinase in vitro (45), although it remains unclear whether these sites contribute to Sml1 phosphorylation and degradation in vivo. We have shown

that deleting residues 28 to 50 of Sml1 while leaving S56/S58/S60 intact drastically increases static protein levels of Sml1. Likewise, deletion of the corresponding region in Dif1 also abolishes phosphorylation-mediated mobility change on SDS-PAGE and degradation of the protein in cells after MMS treatment. Our results indicate that the homologous region shared by Dif1 and Sml1 is involved in DNA damage-induced phosphorylation and degradation of the two proteins. It is possible that multiple and redundant serine/threonine residues within this region can be substrates of the checkpoint kinase(s) and that a gradual increase in overall phosphorylation levels in the region eventually triggers a conformational change in the protein to be recognized by the protein degradation machinery.

The location and mechanistic details of protein degradation of Sml1 are unknown. *S. pombe* Spd1 is degraded in the nucleus by the Cop9/signalosome (29). Because of the proximity of the checkpoint kinases to chromatin (10, 23), Dif1 phosphorylation is likely to occur in the nucleus. Considering its small size and stoichiometric levels relative to R2, we hypothesize that Dif1 readily shuttles back to the cytoplasm after helping import R2 into the nucleus and delivering it to Wtm1. The basal level of checkpoint kinase-mediated phosphorylation and degradation of Dif1 in the nucleus can help explain the absence of the protein in the nucleus fraction. When cells encounter genotoxic stress, checkpoint kinases become hyperactive, ultimately leading to accumulation of phosphorylated Dif1 protein, as detected in the nucleus.

A conserved family of small protein regulators of RNR. Dif1 appears to be a hybrid between *S. cerevisiae* Sml1 and *S. pombe* Spd1. No readily identifiable sequence homolog of Sml1 is found in *S. pombe*, and likewise, no Spd1 ortholog is found in *S. cerevisiae*. Interestingly, while orthologs of *SML1* can be found only in close relatives of *S. cerevisiae*, counterparts of *DIF1* exist in more distantly related fungal genomes like *Kluyveromyces* and *Candida*. In fact, these distant relatives of *S. cerevisiae* appear to have only Dif1 but no Sml1 or Spd1 counterparts. These findings raise intriguing questions of how these small proteins may have arisen during evolution in controlling RNR activities and cellular dNTP pools. We speculate that some Dif1 homologs function more like Spd1 in controlling R2 localization while others function more like Sml1 in inhibition of R1. Molecular characterization of the Dif1-RNR interaction will serve as the starting point for addressing this and other important questions about the regulation of RNR activity and cellular dNTP pool sizes. A better mechanistic understanding of these functionally related proteins may also lead to identification of their structural and/or functional counterparts in higher eukaryotes.

ACKNOWLEDGMENTS

We thank Xiuxiang An for excellent technical assistance.

This work was supported by a grant from the National Institutes of Health (CA125574) to M.H.

REFERENCES

- Allen, J. B., Z. Zhou, W. Siede, E. C. Friedberg, and S. J. Elledge. 1994. The SAD1/RAD53 protein kinase controls multiple checkpoints and DNA damage-induced transcription in yeast. *Genes Dev.* **8**:2401–2415.
- An, X., Z. Zhang, K. Yang, and M. Huang. 2006. Cotransport of the heterodimeric small subunit of the *Saccharomyces cerevisiae* ribonucleotide reductase between the nucleus and the cytoplasm. *Genetics* **173**:63–73.
- Bitter, G. A., K. K. Chang, and K. M. Egan. 1991. A multi-component upstream activation sequence of the *Saccharomyces cerevisiae* glyceraldehyde-3-phosphate dehydrogenase gene promoter. *Mol. Gen. Genet.* **231**:22–32.
- Bondar, T., A. Ponomarev, and P. Raychaudhuri. 2004. Ddb1 is required for the proteolysis of the *Schizosaccharomyces pombe* replication inhibitor Spd1 during S phase and after DNA damage. *J. Biol. Chem.* **279**:9937–9943.
- Brachmann, C. B., A. Davies, G. J. Cost, E. Caputo, J. Li, P. Hieter, and J. D. Boeke. 1998. Designer deletion strains derived from *Saccharomyces cerevisiae* S288C: a useful set of strains and plasmids for PCR-mediated gene disruption and other applications. *Yeast* **14**:115–132.
- Burke, D., D. Dawson, and T. Stearns. 2000. *Methods in yeast genetics: a Cold Spring Harbor Laboratory course manual*, 2000 edition. Cold Spring Harbor Laboratory Press, Cold Spring Harbor, NY.
- Chabes, A., V. Domkin, G. Larsson, A. Liu, A. Graslund, S. Wijmenga, and L. Thelander. 2000. Yeast ribonucleotide reductase has a heterodimeric iron-radical-containing subunit. *Proc. Natl. Acad. Sci. USA* **97**:2474–2479.
- Chabes, A., V. Domkin, and L. Thelander. 1999. Yeast Sml1, a protein inhibitor of ribonucleotide reductase. *J. Biol. Chem.* **274**:36679–36683.
- Chabes, A. L., C. M. Pfleger, M. W. Kirschner, and L. Thelander. 2003. Mouse ribonucleotide reductase R2 protein: a new target for anaphase-promoting complex-Cdh1-mediated proteolysis. *Proc. Natl. Acad. Sci. USA* **100**:3925–3929.
- Cobb, J. A., L. Bjergbaek, K. Shimada, C. Frei, and S. M. Gasser. 2003. DNA polymerase stabilization at stalled replication forks requires Mec1 and the RecQ helicase Sgs1. *EMBO J.* **22**:4325–4336.
- Craven, R. J., P. W. Greenwell, M. Dominska, and T. D. Petes. 2002. Regulation of genome stability by TEL1 and MEC1, yeast homologs of the mammalian ATM and ATR genes. *Genetics* **161**:493–507.
- Davidson, J. D., L. Ma, M. Flagella, S. Geeganage, L. M. Gelbert, and C. A. Slapak. 2004. An increase in the expression of ribonucleotide reductase large subunit 1 is associated with gemcitabine resistance in non-small cell lung cancer cell lines. *Cancer Res.* **64**:3761–3766.
- Desany, B. A., A. A. Alcasabas, J. B. Bachant, and S. J. Elledge. 1998. Recovery from DNA replicational stress is the essential function of the S-phase checkpoint pathway. *Genes Dev.* **12**:2956–2970.
- Fox, S. A., S. Loh, A. L. Thean, and M. J. Garlepp. 2004. Identification of differentially expressed genes in murine mesothelioma cell lines of differing tumorigenicity using suppression subtractive hybridization. *Biochim. Biophys. Acta* **1688**:237–244.
- Gasch, A. P., M. Huang, S. Metzner, D. Botstein, S. J. Elledge, and P. O. Brown. 2001. Genomic expression responses to DNA-damaging agents and the regulatory role of the yeast ATR homolog Mec1p. *Mol. Biol. Cell* **12**:2987–3003.
- Hakansson, P., L. Dahl, O. Chilkova, V. Domkin, and L. Thelander. 2006. The *Schizosaccharomyces pombe* replication inhibitor Spd1 regulates ribonucleotide reductase activity and dNTPs by binding to the large Cdc22 subunit. *J. Biol. Chem.* **281**:1778–1783.
- Huang, M., and S. J. Elledge. 1997. Identification of *RNR4*, encoding a second essential small subunit of ribonucleotide reductase in *Saccharomyces cerevisiae*. *Mol. Cell. Biol.* **17**:6105–6113.
- Huang, M., Z. Zhou, and S. J. Elledge. 1998. The DNA replication and damage checkpoint pathways induce transcription by inhibition of the Crt1 repressor. *Cell* **94**:595–605.
- Huh, W. K., J. V. Falvo, L. C. Gerke, A. S. Carroll, R. W. Howson, J. S. Weissman, and E. K. O'Shea. 2003. Global analysis of protein localization in budding yeast. *Nature* **425**:686–691.
- Jordan, A., and P. Reichard. 1998. Ribonucleotide reductases. *Annu. Rev. Biochem.* **67**:71–98.
- Kashlan, O. B., and B. S. Cooperman. 2003. Comprehensive model for allosteric regulation of mammalian ribonucleotide reductase: refinements and consequences. *Biochemistry* **42**:1696–1706.
- Kimura, T., S. Takeda, Y. Sagiya, M. Gotoh, Y. Nakamura, and H. Arakawa. 2003. Impaired function of p53R2 in Rrm2b-null mice causes severe renal failure through attenuation of dNTP pools. *Nat. Genet.* **34**:440–445.
- Kondo, T., T. Wakayama, T. Naiki, K. Matsumoto, and K. Sugimoto. 2001. Recruitment of Mec1 and Ddc1 checkpoint proteins to double-strand breaks through distinct mechanisms. *Science* **294**:867–870.
- Koshland, D., J. C. Kent, and L. H. Hartwell. 1985. Genetic analysis of the mitotic transmission of minichromosomes. *Cell* **40**:393–403.
- Kuo, M. L., H. S. Hwang, P. R. Sosnay, K. A. Kunugi, and T. J. Kinsella. 2003. Overexpression of the R2 subunit of ribonucleotide reductase in human nasopharyngeal cancer cells reduces radiosensitivity. *Cancer J.* **9**:277–285.
- Lee, Y. D., and S. J. Elledge. 2006. Control of ribonucleotide reductase localization through an anchoring mechanism involving Wtm1. *Genes Dev.* **20**:334–344.
- Lee, Y. D., J. Wang, J. Stubbe, and S. J. Elledge. 2008. Dif1 is a DNA damage regulated facilitator of nuclear import for ribonucleotide reductase. *Mol. Cell* **32**:70–80.
- Lincker, F., G. Philipps, and M. E. Chaboute. 2004. UV-C response of the ribonucleotide reductase large subunit involves both E2F-mediated gene transcriptional regulation and protein subcellular relocation in tobacco cells. *Nucleic Acids Res.* **32**:1430–1438.

29. Liu, C., K. A. Powell, K. Mundt, L. Wu, A. M. Carr, and T. Caspari. 2003. Cop9/signalosome subunits and Pcu4 regulate ribonucleotide reductase by both checkpoint-dependent and -independent mechanisms. *Genes Dev.* **17**: 1130–1140.
30. Liu, X., B. Zhou, L. Xue, J. Shih, K. Tye, C. Qi, and Y. Yen. 2005. The ribonucleotide reductase subunit M2B subcellular localization and functional importance for DNA replication in physiological growth of KB cells. *Biochem. Pharmacol.* **70**:1288–1297.
31. Mann, G. J., E. A. Musgrove, R. M. Fox, and L. Thelander. 1988. Ribonucleotide reductase M1 subunit in cellular proliferation, quiescence, and differentiation. *Cancer Res.* **48**:5151–5156.
32. Nakano, K., E. Balint, M. Ashcroft, and K. H. Vousden. 2000. A ribonucleotide reductase gene is a transcriptional target of p53 and p73. *Oncogene* **19**:4283–4289.
33. Neville, M., and M. Rosbash. 1999. The NES-Crm1p export pathway is not a major mRNA export route in *Saccharomyces cerevisiae*. *EMBO J.* **18**: 3746–3756.
34. Nordlund, P., and P. Reichard. 2006. Ribonucleotide reductases. *Annu. Rev. Biochem.* **75**:681–706.
35. Ortigosa, A. D., D. Hristova, D. L. Perlstein, Z. Zhang, M. Huang, and J. Stubbe. 2006. Determination of the in vivo stoichiometry of tyrosyl radical per betabeta' in *Saccharomyces cerevisiae* ribonucleotide reductase. *Biochemistry* **45**:12282–12294.
36. Perlstein, D. L., J. Ge, A. D. Ortigosa, J. H. Robblee, Z. Zhang, M. Huang, and J. Stubbe. 2005. The active form of the *Saccharomyces cerevisiae* ribonucleotide reductase small subunit is a heterodimer in vitro and in vivo. *Biochemistry* **44**:15366–15377.
37. Rofougaran, R., M. Vodnala, and A. Hofer. 2006. Enzymatically active mammalian ribonucleotide reductase exists primarily as an alpha6beta2 octamer. *J. Biol. Chem.* **281**:27705–27711.
38. Sanchez, Y., Z. Zhou, M. Huang, B. E. Kemp, and S. J. Elledge. 1997. Analysis of budding yeast kinases controlled by DNA damage. *Methods Enzymol.* **283**:398–410.
39. Schimmang, T., D. Tollervey, H. Kern, R. Frank, and E. C. Hurt. 1989. A yeast nucleolar protein related to mammalian fibrillarin is associated with small nucleolar RNA and is essential for viability. *EMBO J.* **8**:4015–4024.
40. Sjoberg, B. M., P. Reichard, A. Graslund, and A. Ehrenberg. 1978. The tyrosine free radical in ribonucleotide reductase from *Escherichia coli*. *J. Biol. Chem.* **253**:6863–6865.
41. Sommerhalter, M., W. C. Voegtli, D. L. Perlstein, J. Ge, J. Stubbe, and A. C. Rosenzweig. 2004. Structures of the yeast ribonucleotide reductase Rnr2 and Rnr4 homodimers. *Biochemistry* **43**:7736–7742.
42. Stubbe, J. 2003. Di-iron-tyrosyl radical ribonucleotide reductases. *Curr. Opin. Chem. Biol.* **7**:183–188.
43. Takahashi, S., K. Kontani, Y. Araki, and T. Katada. 2007. Caf1 regulates translocation of ribonucleotide reductase by releasing nucleoplasmic Spd1-Suc22 assembly. *Nucleic Acids Res.* **35**:1187–1197.
44. Tanaka, H., H. Arakawa, T. Yamaguchi, K. Shiraishi, S. Fukuda, K. Matsui, Y. Takei, and Y. Nakamura. 2000. A ribonucleotide reductase gene involved in a p53-dependent cell-cycle checkpoint for DNA damage. *Nature* **404**: 42–49.
45. Uchiki, T., L. T. Dice, R. L. Hettich, and C. Dealwis. 2004. Identification of phosphorylation sites on the yeast ribonucleotide reductase inhibitor Sml1. *J. Biol. Chem.* **279**:11293–11303.
46. Voegtli, W. C., J. Ge, D. L. Perlstein, J. Stubbe, and A. C. Rosenzweig. 2001. Structure of the yeast ribonucleotide reductase Y2Y4 heterodimer. *Proc. Natl. Acad. Sci. USA* **98**:10073–10078.
47. Wang, J., G. J. Lohman, and J. Stubbe. 2007. Enhanced subunit interactions with gemcitabine-5'-diphosphate inhibit ribonucleotide reductases. *Proc. Natl. Acad. Sci. USA* **104**:14324–14329.
48. Wang, P. J., A. Chabes, R. Casagrande, X. C. Tian, L. Thelander, and T. C. Huffaker. 1997. Rnr4p, a novel ribonucleotide reductase small-subunit protein. *Mol. Cell. Biol.* **17**:6114–6121.
49. Woollard, A., G. Basi, and P. Nurse. 1996. A novel S phase inhibitor in fission yeast. *EMBO J.* **15**:4603–4612.
50. Yao, R., Z. Zhang, X. An, B. Bucci, D. L. Perlstein, J. Stubbe, and M. Huang. 2003. Subcellular localization of yeast ribonucleotide reductase regulated by the DNA replication and damage checkpoint pathways. *Proc. Natl. Acad. Sci. USA* **100**:6628–6633.
51. Zhang, Z., X. An, K. Yang, D. L. Perlstein, L. Hicks, N. Kelleher, J. Stubbe, and M. Huang. 2006. Nuclear localization of the *Saccharomyces cerevisiae* ribonucleotide reductase small subunit requires a karyopherin and a WD40 repeat protein. *Proc. Natl. Acad. Sci. USA* **103**:1422–1427.
52. Zhao, X., A. Chabes, V. Domkin, L. Thelander, and R. Rothstein. 2001. The ribonucleotide reductase inhibitor Sml1 is a new target of the Mec1/Rad53 kinase cascade during growth and in response to DNA damage. *EMBO J.* **20**:3544–3553.
53. Zhao, X., B. Georgieva, A. Chabes, V. Domkin, J. H. Ippel, J. Schleucher, S. Wijmenga, L. Thelander, and R. Rothstein. 2000. Mutational and structural analyses of the ribonucleotide reductase inhibitor Sml1 define its Rnr1 interaction domain whose inactivation allows suppression of *mecl1* and *rad53* lethality. *Mol. Cell. Biol.* **20**:9076–9083.
54. Zhao, X., E. G. Muller, and R. Rothstein. 1998. A suppressor of two essential checkpoint genes identifies a novel protein that negatively affects dNTP pools. *Mol. Cell* **2**:329–340.
55. Zhao, X., and R. Rothstein. 2002. The Dun1 checkpoint kinase phosphorylates and regulates the ribonucleotide reductase inhibitor Sml1. *Proc. Natl. Acad. Sci. USA* **99**:3746–3751.
56. Zhou, B., X. Mo, X. Liu, W. Qiu, and Y. Yen. 2001. Human ribonucleotide reductase M2 subunit gene amplification and transcriptional regulation in a homogeneous staining chromosome region responsible for the mechanism of drug resistance. *Cytogenet. Cell Genet.* **95**:34–42.